

# An Approach to Fuzzy Modeling of Magnetic Levitation Systems

Radu-Codrut David<sup>1</sup>, Claudia-Adina Dragoş<sup>1</sup>, Raul-Gherasim Bulzan<sup>1</sup>,  
Radu-Emil Precup<sup>1</sup>, Emil M. Petriu<sup>2</sup>, Mircea-Bogdan Radac<sup>1</sup>

<sup>1</sup>Dept. of Automation and Applied Informatics, "Politehnica" University of Timisoara,

Bd. V. Parvan 2, 300223 Timisoara, Romania;

davidradu@gmail.com, claudia.dragos@aut.upt.ro, braul\_roxi@yahoo.com,  
radu.precup@aut.upt.ro, mircea.radac@aut.upt.ro

<sup>2</sup>University of Ottawa, School of Electrical Engineering and Computer Science,

800 King Edward, Ottawa, ON, K1N 6N5 Canada;

petriu@eecs.uottawa.ca

## ABSTRACT

*This paper proposes an approach to fuzzy modeling of magnetic levitation systems. These unstable and nonlinear processes are first linearized around several operating points, and next stabilized by a State Feedback Control System (SFCS) structure. Discrete-time Takagi-Sugeno (T-S) fuzzy models of the stabilized processes are derived on the basis of the modal equivalence principle, and the rule consequents contain the state-space models of the local SFCS structures. Optimization problems are defined which aim the minimization of objective functions defined as the squared modeling error considered as the difference between the real-world process output and the fuzzy model output. The variables of the objective functions are represented by a part of the parameters of the input membership functions. Simulated Annealing algorithms are implemented to solve these optimization problems and to obtain optimal T-S fuzzy models. Real-time experimental results validate the fuzzy modeling approach and the new optimal T-S fuzzy models for a Magnetic Levitation System with Two Electromagnets (MLS2EM) laboratory equipment.*

**Keywords:** Takagi-Sugeno fuzzy models, magnetic levitation system, real-time experiments, optimization, simulated annealing.

**Mathematics Subject Classification:** 82C21, 93A30

**Computing Classification System:** I.2.3, I.2.9

## 1. INTRODUCTION

The process taken into consideration and modeled in this paper is a complete laboratory system based on the Magnetic Levitation System with Two Electromagnets (MLS2EM) (Inteco, 2008). The magnetic levitation problem for a metallic sphere maintained in an electromagnetic field is a classical nonlinear and unstable application. Therefore the derivation of optimal Takagi-Sugeno (T-S) fuzzy models is a challenging problem.

In this paper, a state-feedback control solution is first designed such that to guarantee the stability of the sphere. Other state-feedback control solutions are designed in literature. A state-feedback control scheme based on the alphabeta filter for controlling the magnetic levitation system or a disturbance observer merged into the K-filter-based output-feedback controller can be used to cancel the external disturbances and model mismatch as discussed in (Lee et al., 2007a) and (Yang et al., 2009). High gain adaptive output feedback controllers and robust stabilizing controllers for magnetic levitation systems are designed in (Michino et al., 2009) and (Satoh et al., 2009).

Second, a discrete-time dynamic T-S fuzzy model of the process is derived in this paper. This derivation starts with the continuous-time models which are obtained on the basis of the local linearization of the process models at nine operating points. The local models are next discretized accepting a zero-order hold and placed in the rule consequents of the T-S fuzzy model of the process.

Several approaches to fuzzy modeling of magnetic levitation systems are given in the literature. They can be viewed in the general framework of fuzzy models with several process (Baranyi et al., 2003), (Škrjanc et al., 2005), (Haber et al., 2010), (Johanyák, 2010), (Vaščák and Madarász, 2010), (Babu Devasenapati and Ramachandran, 2011), (Xi et al., 2011). The nonlinear dynamic equations of the magnetic levitation systems are represented in (Yu and Huang, 2009) by a T-S fuzzy model; the optimal gains are found by using particle swarm optimization and quantum-inspired evolutionary algorithms. In order to model the nonlinear magnetic bearing systems, a linear T-S fuzzy model is proposed in (Yu et al., 2003); this model is obtained using a linear self-constructing neural fuzzy inference network applied to an optimal fuzzy controller, which can operate in a widely range of shaft positions. A T-S fuzzy model for nonlinear magnetic bearing systems is offered in (Hong et al., 1997). A fuzzy neural network modeling approach is proposed in (Yongzhi et al., 2011) to model gap sensor in high-speed maglev trains; this model-based fuzzy network scheme incorporates intelligence into the sensor, which can estimate the correct true gap in a range of temperature after proper training. A design method of parallel distributed compensation controller based on T-S fuzzy models for magnetic bearing of high-speed motors is proposed in (Wang and Wang, 2010).

A Simulated Annealing (SA) algorithm is used in order to get optimal T-S fuzzy models for the process aiming high performance fuzzy control systems as a future step. This algorithm will optimize the parameters of the T-S fuzzy model in the context of an appropriately defined optimization problem which aims the minimization of an objective function targeting a small difference between process's output (i.e., the sphere position) and T-S fuzzy model's output. The new SA algorithm proposed in this

paper can be considered in the context of many evolutionary-based nature-inspired optimization algorithms employed in the numerical solving of various optimization problems for specific objective functions. An SA algorithm is used to optimize the fuzzy controller parameters in angular position control of DC servo systems (Precup et al., 2011b). Genetic algorithms are applied to the optimization of parameters of switch reluctance motors (Xiu and Xia, 2007). A real-coded genetic algorithm is used to simultaneously adjust both the membership functions and model parameters in the consequents of T-S fuzzy models (Lee et al., 2007b).

This paper offers a relatively simple approach to fuzzy modeling of magnetic levitation systems. Our approach starts with the derivation of an initial T-S fuzzy model of the process obtained by the modal equivalence principle; this fuzzy model is characterized by a set of local linearized state-space models of the process which are placed in the rule consequents. A part of the parameters of the input membership functions is next optimized by our SA algorithm in order to solve the optimization problems which aim the minimization of the sum of squared modeling errors. The discrete-time treatment of models is carried out.

The main advantage of our approach is that the performance of the optimal T-S fuzzy model is verified through by real-time experiments on the MLS2EM laboratory equipment and not only by simulation. Although our approach cannot guarantee that the global minimum of the objective functions is reached, it is shown that a serious decrease of the objective function is exhibited, and this clearly indicates the performance improvement offered by our T-S fuzzy model.

The paper is organized as follows. Section 2 is dedicated to the mathematical modeling of the process and to the design of T-S fuzzy models. The main aspects concerning the implementation of our SA algorithm are discussed in Section 3. Real-time experimental results are presented in Section 4 to validate the new optimal T-S fuzzy models. The concluding remarks are highlighted in Section 5.

## **2. FUZZY MODELS OF MLS2EM PROCESS**

### **2.1 Process Modeling**

The block diagram of the ML2SEM considered as a controlled process is presented in Figure 1, where EM1, EM2 are the upper and lower electromagnet,  $m$  is the mass of the sphere,  $F_{em1}$  and  $F_{em2}$  are the electromagnetic forces, and  $F_g$  is the gravity force (Inteco, 2008).

Our approach starts with the modeling of the nonlinear MLS2EM which can be obtained from the following first principle equations:

$$\begin{aligned}
\dot{x}_1 &= x_2, \\
\dot{x}_2 &= -\frac{1}{m} \cdot \frac{F_{emP1}}{F_{emP2}} \cdot e^{-\frac{x_1}{F_{emP1}}} \cdot x_3^2 + g + \frac{1}{m} \cdot \frac{F_{emP1}}{F_{emP2}} \cdot e^{-\frac{x_d - x_1}{F_{emP2}}} \cdot x_4^2, \\
\dot{x}_3 &= \frac{1}{\frac{f_{iP1}}{f_{iP2}} \cdot e^{-\frac{x_1}{f_{iP2}}}} (k_i u_1 + c_i - x_3), \\
\dot{x}_4 &= \frac{1}{\frac{f_{iP1}}{f_{iP2}} \cdot e^{-\frac{x_d - x_1}{f_{iP2}}}} (k_i u_2 + c_i - x_4), \\
y &= x_1,
\end{aligned} \tag{1}$$

where the characteristic variables are:

- the control signal  $u_1$ , which is applied to the upper electromagnet (EM1),
- the disturbance input  $d = u_2$ , which is applied to the lower electromagnet (EM2),
- the state variables:  $x_1$  is the sphere position,  $x_2$  is the sphere speed,  $x_3$  and  $x_4$  are the currents in the upper and lower electromagnetic coil, respectively;
- the controlled output (output variable)  $y = x_1$ .

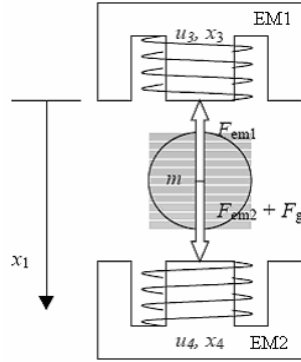


**Figure 1.** Block diagram of ML2SEM.

The numerical values of the parameters are given in (Inteco, 2008).

Due to the nonlinearities of the systems, we are carrying out the linearization of the nonlinear model (1) at nine operating points  $A_j(x_{10}, x_{20}, x_{30}, x_{40})$  (with  $j$  – the index of the operating point) to meet the fuzzy models. Therefore, the linearized state-space models are:

$$\begin{cases} \dot{\underline{x}} = \underline{A} \underline{x} + \underline{B} \Delta u \\ y = \underline{c}^T \underline{x} \end{cases}, \underline{x} = \begin{bmatrix} \Delta x_1 \\ \Delta x_2 \\ \Delta x_3 \\ \Delta x_4 \end{bmatrix}, \quad (2)$$

$$\underline{A} = \begin{bmatrix} 0 & 1 & 0 & 0 \\ a_{2,1} & 0 & a_{2,3} & a_{2,4} \\ a_{3,1} & 0 & a_{3,3} & 0 \\ a_{4,1} & 0 & 0 & a_{4,4} \end{bmatrix}, \underline{b} = \begin{bmatrix} 0 \\ 0 \\ b_3 \\ b_4 \end{bmatrix}, \underline{c}^T = [1 \ 0 \ 0 \ 0]$$

and the matrix elements are:

$$\begin{aligned} a_{11} &= 0, a_{12} = 1, a_{13} = 0, a_{14} = 0, \\ a_{21} &= \frac{x_{30}^2}{m} \frac{F_{emP1}}{F_{emP2}^2} e^{-\frac{x_{10}}{F_{emP2}}} + \frac{x_{40}^2}{m} \frac{F_{emP1}}{F_{emP2}^2} e^{-\frac{x_d - x_{10}}{F_{emP2}}}, a_{22} = 0, \\ a_{23} &= -\frac{2x_{30}}{m} \frac{F_{emP1}}{F_{emP2}} e^{-\frac{x_{10}}{F_{emP2}}}, a_{24} = \frac{2x_{40}}{m} \frac{F_{emP1}}{F_{emP2}} e^{-\frac{x_d - x_{10}}{F_{emP2}}} \\ a_{31} &= \frac{f_{iP2}}{f_{iP1}} \cdot e^{\frac{x_{10}}{f_{iP2}}} \cdot (k_i u_1 + c_i - x_{30}), a_{32} = 0, a_{33} = -\frac{1}{f_{iP1}} \cdot e^{\frac{x_{10}}{f_{iP2}}}, a_{34} = 0 \\ a_{41} &= -\frac{1}{f_{iP1}} \cdot e^{\frac{x_d - x_{10}}{F_{emP2}}} \cdot (k_i u_2 + c_i - x_{40}), \\ a_{42} &= 0, a_{43} = 0, a_{44} = -\frac{f_{iP2}}{f_{iP1}} \cdot e^{\frac{x_d - x_{10}}{F_{emP2}}} \\ b_{11} &= 0, b_{21} = 0, b_{31} = k_i \cdot \frac{f_{iP2}}{f_{iP1}} \cdot e^{\frac{x_{10}}{f_{iP2}}}, b_{41} = k_i \cdot \frac{f_{iP2}}{f_{iP1}} \cdot e^{\frac{x_d - x_{10}}{F_{emP2}}} \end{aligned} \quad (3)$$

The fourth-order model detailed in equation (1) is next reduced to the following third order state-space model of the MLS2EM which is obtained in terms of neglecting the lower electromagnet,  $u_2 = 0$ :

$$\begin{cases} \dot{\underline{x}} = \underline{A} \underline{x} + \underline{B} \Delta u \\ y = \underline{c}^T \underline{x} \end{cases}, \underline{x} = \begin{bmatrix} \Delta x_1 \\ \Delta x_2 \\ \Delta x_3 \end{bmatrix}, \quad (4)$$

$$\underline{A} = \begin{bmatrix} 0 & 1 & 0 \\ a_{21} & 0 & a_{23} \\ a_{31} & 0 & a_{33} \end{bmatrix}, \underline{B} = \begin{bmatrix} 0 \\ 0 \\ b_3 \end{bmatrix}, \underline{c}^T = [1 \ 0 \ 0]$$

The parameters of the matrices  $\underline{A}, \underline{b}, \underline{c}^T$  are:

$$\begin{aligned}
a_{2,1} &= \frac{x_{30}^2}{m} \frac{F_{emP1}}{F_{emP2}^2} e^{-\frac{x_{10}}{F_{emP2}}} + \frac{x_{40}^2}{m} \frac{F_{emP1}}{F_{emP2}^2} e^{-\frac{x_d - x_{10}}{F_{emP2}}}, \\
a_{2,3} &= -\frac{2x_{30}}{m} \frac{F_{emP1}}{F_{emP2}} e^{-\frac{x_{10}}{F_{emP2}}}, \\
a_{3,1} &= -(k_i u + c_i - x_{30})(x_{10} / f_{iP2}) f_i^{-1}(x_{10}), \quad a_{3,3} = -f_i^{-1}(x_{10}), \\
b_3 &= k_i f_i^{-1}(x_{10}).
\end{aligned} \tag{5}$$

In order to stabilize the sphere in the MLS2EM, a state-feedback control structure is designed. First, the closed-loop system poles detailed in Table I are imposed. The pole placement method is used to obtain the state-feedback gain matrix:

$$\underline{k}_c^T = [36 \quad 5 \quad 0.0075]. \tag{6}$$

Therefore the following closed third order continuous-time state-space linearised model is obtained:

$$\begin{cases} \dot{\underline{x}} = \underline{A}_x \underline{x} + \underline{b} r_x \\ \underline{y} = \underline{c}^T \underline{x} \end{cases}, \quad \underline{x} = [\Delta x_1 \quad \Delta x_2 \quad \Delta x_3]^T, \tag{7}$$

where the numerical values of the matrices  $\underline{A}_x, \underline{b}_u, \underline{c}^T$  in discrete time are detailed in Table I.

TABLE I. NUMERICAL VALUES OF MATRICES IN DISCRETE-TIME LINEARIZED THIRD-ORDER MODELS OF CLOSED-LOOP STABILIZED ML2SEM

Operating points	Closed-loop system poles			Numerical values of the matrices in discrete Time	
	$P_1^*$	$P_2^*$	$P_3^*$		
$x_{10} = 0.007;$ $x_{20} = 0;$ $x_{30} = 0.285;$ $x_{40} = 0;$	-15.64	-65.58-102.09i	-65.58+102.09i	$A_{d1} = \begin{bmatrix} 0.9982 & 0.0047 & -0.00009 \\ -1.482 & 0.8350 & -0.02977 \\ 99.96 & 6.488 & 0.3488 \end{bmatrix};$	$B_{d1} = \begin{bmatrix} -0.00006 \\ -0.03263 \\ 1.24 \end{bmatrix};$
$x_{10} = 0.007;$ $x_{20} = 0;$ $x_{30} = 0.6;$ $x_{40} = 0;$	-6.28	-70.26-170.24i	-70.26+170.24i	$A_{d2} = \begin{bmatrix} 1.005 & 0.0044 & -0.00017 \\ 1.014 & 0.6741 & -0.05798 \\ 74.35 & 5.918 & 0.2172 \end{bmatrix};$	$B_{d2} = \begin{bmatrix} -0.00012 \\ -0.06628 \\ 1.143 \end{bmatrix};$
$x_{10} = 0.008;$ $x_{20} = 0;$ $x_{30} = 0.3;$ $x_{40} = 0;$	-15.50	-83.64-94.68i	-83.64+94.68i	$A_{d3} = \begin{bmatrix} 0.9978 & 0.0047 & -0.00007 \\ -1.623 & 0.8274 & -0.02424 \\ 112.3 & 7.423 & 0.2719 \end{bmatrix};$	$B_{d3} = \begin{bmatrix} -0.00006 \\ -0.03408 \\ 1.418 \end{bmatrix};$
$x_{10} = 0.008;$ $x_{20} = 0;$ $x_{30} = 0.6;$ $x_{40} = 0;$	-6.28	-88.25-166.73i	-88.25+166.73i	$A_{d4} = \begin{bmatrix} 1.004 & 0.0044 & -0.00014 \\ 0.3517 & 0.6747 & -0.04484 \\ 82.42 & 6.771 & 0.3488 \end{bmatrix};$	$B_{d4} = \begin{bmatrix} -0.00012 \\ -0.06578 \\ 1.307 \end{bmatrix};$
$x_{10} = 0.009;$ $x_{20} = 0;$ $x_{30} = 0.3;$ $x_{40} = 0;$	-16.13	-105.72-70.08i	-105.72+70.08i	$A_{d5} = \begin{bmatrix} 0.9974 & 0.0047 & -0.00006 \\ -1.733 & 0.8298 & -0.01854 \\ 126.3 & 8.403 & 0.2026 \end{bmatrix};$	$B_{d5} = \begin{bmatrix} -0.00006 \\ -0.03352 \\ 1.603 \end{bmatrix};$

$x_{10} = 0.009;$ $x_{20} = 0;$ $x_{30} = 0.285;$ $x_{40} = 0;$	-16.92	-105.32-62.25i	-105.32+62.25i	$A_{d6} = \begin{bmatrix} 0.9974 & 0.0047 & -0.00006 \\ -1.729 & 0.8378 & -0.01768 \\ 128.5 & 8.443 & 0.2082 \end{bmatrix}; B_{d6} = \begin{bmatrix} -0.00006 \\ -0.03191 \\ 1.61 \end{bmatrix};$ $C_{d6} = [1 \ 0 \ 0]; D_{d6} = 0;$
$x_{10} = 0.007;$ $x_{20} = 0;$ $x_{30} = 0.3;$ $x_{40} = 0;$	-15.07	-65.87-106.41i	-65.87+106.41i	$A_{d7} = \begin{bmatrix} 0.9983 & 0.0047 & -0.00009 \\ -1.457 & 0.8268 & -0.03122 \\ 98.41 & 6.459 & 0.3422 \end{bmatrix}; B_{d7} = \begin{bmatrix} -0.00006 \\ -0.03429 \\ 1.235 \end{bmatrix};$ $C_{d7} = [1 \ 0 \ 0]; D_{d7} = 0;$
$x_{10} = 0.008;$ $x_{20} = 0;$ $x_{30} = 0.285;$ $x_{40} = 0;$	-16.16	83.31-89.46i	-83.31+89.46i	$A_{d8} = \begin{bmatrix} 0.9977 & 0.0047 & -0.00006 \\ -1.632 & 0.8355 & -0.03122 \\ 114.1 & 7.457 & 0.2781 \end{bmatrix}; B_{d8} = \begin{bmatrix} -0.00006 \\ -0.0344 \\ 1.424 \end{bmatrix};$ $C_{d8} = [1 \ 0 \ 0]; D_{d8} = 0;$
$x_{10} = 0.009;$ $x_{20} = 0;$ $x_{30} = 0.6;$ $x_{40} = 0;$	-6.29	-110.64-158.17i	-110.64+158.17i	$A_{d9} = \begin{bmatrix} 1.002 & 0.0044 & -0.00011 \\ -0.1642 & 0.679 & -0.03415 \\ 90.37 & 7.633 & 0.09682 \end{bmatrix}; B_{d9} = \begin{bmatrix} -0.00012 \\ -0.06461 \\ 1.472 \end{bmatrix};$ $C_{d9} = [1 \ 0 \ 0]; D_{d9} = 0;$

## 2.2 Approach to Takagi-Sugeno Fuzzy Modeling

In order to capture both the static nonlinearity and the linear dynamics of the process, the derivation of a discrete-time dynamic T-S fuzzy model of the process is presented as follows. The steps of our modeling approach are:

- definition of the membership functions of the input variables  $x_1$  and  $x_3$ ,
- derivation of an initial T-S fuzzy model of the process, which has the state variables  $x_1$  and  $x_3$  as input variables, and the discrete-time state-space models of the process with the matrices  $\mathbf{A}_{d,i}$ ,  $\mathbf{B}_{d,i}$  and  $\mathbf{C}_{d,i}$ ,  $i = \overline{1,9}$ , in the rule consequents,
- definition of optimization problem where the vector variable of the objective function consists of a part of the parameters of the input membership functions of the T-S fuzzy model,
- application of SA algorithm to obtain the optimal input membership function parameters which lead to the optimal dynamic T-S fuzzy model.

The derivation of the initial T-S fuzzy model starts with the setting of the largest domains of variation of the two state variables uses in all MLS2EM operating regimes:

$$-0.2 \leq x_1 \leq 0.2, -8.757 \leq x_3 \leq 18.765. \quad (8)$$

The fuzzification part of the T-S fuzzy model consists of the linguistic terms assigned to the input variables and defined as follows. For the input variable  $x_1$ , three linguistic terms,  $TL_{x_1,j}$ ,  $j = \overline{1,3}$ , with triangular membership functions are defined and referred to as  $TL_{x_1,1}$ , with the universe of discourse  $[-0.2 \ 0]$ ,  $TL_{x_1,2}$ , with the universe of discourse  $[-0.1 \ 0.1]$ , and  $TL_{x_1,3}$ , with the universe of

discourse  $[0 \ 0.2]$ . The expressions of these triangular membership functions are:

$$\mu_{TL_{x_1,j}}(x) = \begin{cases} 0, & x < a_{x_1,j} \\ 1 + \frac{x - b_{x_1,j}}{b_{x_1,j} - a_{x_1,j}}, & x \in [a_{x_1,j}, b_{x_1,j}) \\ 1 - \frac{x - b_{x_1,j}}{c_{x_1,j} - b_{x_1,j}}, & x \in [b_{x_1,j}, c_{x_1,j}) \\ 0, & x \geq c_{x_1,j} \end{cases}, \quad a_{x_1,j} < b_{x_1,j} < c_{x_1,j}, \quad j = \overline{1,3}, \quad (9)$$

where the initial modal values of the membership functions are the parameters  $a_{x_1,j}$ ,  $b_{x_1,j}$ , and  $c_{x_1,j}$ ,  $j = \overline{1,3}$ , given in Table II. The parameters  $a_{x_1,j}$ ,  $j = \overline{1,3}$  and  $c_{x_1,j}$ ,  $j = \overline{1,3}$  are fixed, and the parameters  $b_{x_1,j}$ ,  $j = \overline{1,3}$  are variable.

TABLE II. MODAL VALUES OF THE LINGUISTIC TERMS

Linguistic terms, $TL_{x_1,j}$ , $j = \overline{1,3}$	Triangular membership functions		
	$a_{x_1,j}$	$b_{x_1,j}$	$c_{x_1,j}$
$TL_{x_1,1}$	-0.2	-0.1	0
$TL_{x_1,2}$	-0.1	0	0.1
$TL_{x_1,3}$	0	0.1	0.2

For the input variable  $x_3$ , three linguistic terms,  $TL_{x_3,j}$ ,  $j = \overline{1,3}$ , are defined. The first and third one are modeled by trapezoidal membership functions, and the second one is modeled by a Gaussian membership functions. The universes of discourse of the membership functions of these linguistic terms are:  $[-8.757 \ 4.3785]$  for  $TL_{x_3,1}$ ,  $[3.753 \ 4.3785]$  for  $TL_{x_3,2}$ , and  $[4.3785 \ 18.765]$  for  $TL_{x_3,3}$ . The expressions of the trapezoidal membership functions are:

$$\mu_{TL_{x_3,j}}(x) = \begin{cases} 0, & x < a_{x_3,j} \\ 1 + \frac{x - b_{x_3,j}}{b_{x_3,j} - a_{x_3,j}}, & x \in [a_{x_3,j}, b_{x_3,j}) \\ 1, & x \in [b_{x_3,j}, c_{x_3,j}), \quad a_{x_3,j} < b_{x_3,j} \leq c_{x_3,j} < d_{x_3,j}, \quad j \in \{1,3\} \\ 1 - \frac{x - c_{x_3,j}}{d_{x_3,j} - c_{x_3,j}}, & x \in [c_{x_3,j}, d_{x_3,j}) \\ 0, & x \geq d_{x_3,j} \end{cases}. \quad (10)$$

The initial modal values of the membership functions are the parameters  $a_{x_3,j}$ ,  $j \in \{1,3\}$ ,  $b_{x_3,j}$ ,  $j \in \{1,3\}$ ,  $c_{x_3,j}$ ,  $j \in \{1,3\}$ , and  $d_{x_3,j}$ ,  $j \in \{1,3\}$ , given in Table III. The parameters

$a_{x3,j}, j \in \{1,3\}$ ,  $b_{x3,1}$ ,  $c_{x3,3}$  and  $d_{x3,j}, j \in \{1,3\}$  are fixed, and the parameters  $c_{x3,1}$  and  $b_{x3,3}$  are variable.

TABLE III. PARAMETERS OF TRAPEZOIDAL LINGUISTIC TERMS

Linguistic terms, $TL_{x3,j}, j = \{1,3\}$	Trapezoidal membership functions			
	$a_{x3,j}, j = \{1,3\}$	$b_{x3,j}, j = \{1,3\}$	$c_{x3,j}, j = \{1,3\}$	$d_{x3,j}, j = \{1,3\}$
$TL_{x3,1}$	-8.757	-8.757	-1.251	4.3785
$TL_{x3,3}$	4.3785	11.259	18.765	18.765

The expression of the Gaussian membership function is:

$$\mu_{TL_{x3,2}}(x) = e^{-\frac{(x-a_{x3,2})^2}{2b_{x3,2}^2}}. \quad (11)$$

The parameter  $b_{x3,2}$  is fixed, and the parameter  $a_{x3,2}$  is variable. The initial values of these two parameters are  $a_{x3,2} = 4.3785$  and  $b_{x3,2} = 3.753$ .

Figure 2 shows the initial membership functions of  $x_1$  and  $x_3$ .

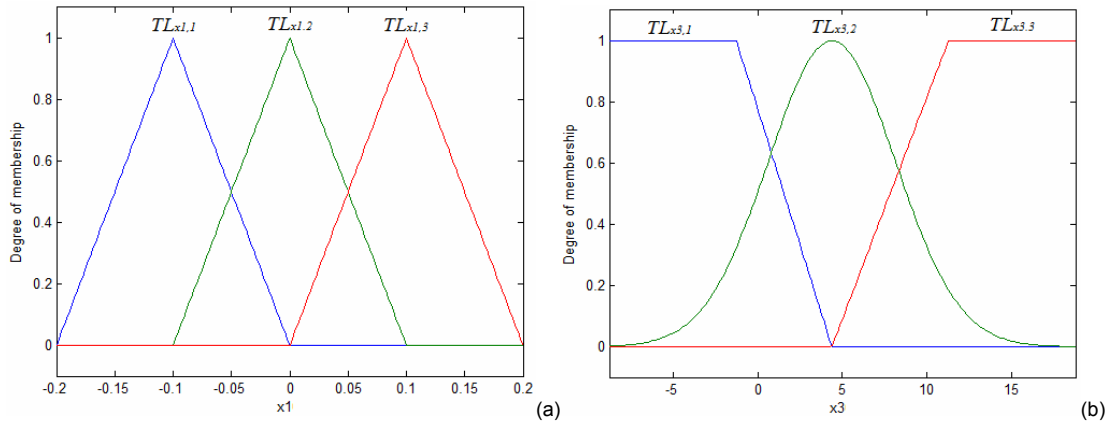


Figure 2. Initial membership functions of the input variables  $x_1$  and  $x_3$ .

The rule consequents correspond to the discrete-time state-space models characterized by the matrices  $\mathbf{A}_{d,i}$ ,  $\mathbf{B}_{d,i}$  and  $\mathbf{C}_{d,i}$ ,  $i = \overline{1,9}$ , detailed in Table II. These models are obtained by discretization of the continuous-time state-space linearized models (5) using the sampling period  $T_s=0.005$  s.

The modal equivalence principle guarantees the equivalence between the fuzzy models and the nonlinear state-space ones. Therefore the rule base of the discrete-time dynamic T-S fuzzy model is expressed as:

$$R^i : \text{IF } z_{1,k} \text{ IS } LT_{z_1,j} \text{ AND } z_{3,k} \text{ IS } LT_{z_3,j} \text{ THEN } \begin{cases} \mathbf{x}_{k+1} = \mathbf{A}_{d,i} \mathbf{x}_k + \mathbf{B}_{d,i} u_k \\ y_{k,m} = \mathbf{C}_{d,i} \mathbf{x}_k \end{cases}, \quad (13)$$

$$i = \overline{1, nR}, j = \overline{1, nLT},$$

where  $k$  stands for the index of the current sampling interval,  $i$  stands for the index of the current rule, and  $j$  stands for the index of the current linguistic terms.

In our case, the complete rule base of the discrete-time dynamic Takagi-Sugeno fuzzy model consists of nine rules  $R^i, i = \overline{1, 9}$ , expressed as:

$$R^1 : \text{IF } z_{1,k} \text{ IS } LT_{z_1,1} \text{ AND } z_{3,k} \text{ IS } LT_{z_3,1}$$

$$\text{THEN } \begin{cases} \mathbf{x}_{k+1} = \mathbf{A}_{d,1} \mathbf{x}_k + \mathbf{B}_{d,1} u_k \\ y_{k,m} = \mathbf{C}_{d,1} \mathbf{x}_k \end{cases}, j = \overline{1, nLT},$$

$$\vdots$$

$$R^9 : \text{IF } z_{1,k} \text{ IS } LT_{z_1,3} \text{ AND } z_{3,k} \text{ IS } LT_{z_3,3}$$

$$\text{THEN } \begin{cases} \mathbf{x}_{k+1} = \mathbf{A}_{d,9} \mathbf{x}_k + \mathbf{B}_{d,9} u_k \\ y_{k,m} = \mathbf{C}_{d,9} \mathbf{x}_k \end{cases}, j = \overline{1, nLT}. \quad (14)$$

The SUM and PROD operators are used in the inference engine, and the weighted average method is employed for defuzzification.

### 3. SIMULATED ANNEALING ALGORITHM

SA is used as a representative nature-inspired biologically-inspired optimization algorithm to solve the optimization problem:

$$\boldsymbol{\rho}^* = \arg \min_{\boldsymbol{\rho} \in D} J(\boldsymbol{\rho}), \quad (15)$$

where  $\boldsymbol{\rho}$  is the parameter vector of the fuzzy model which collects all variable parameters of the membership functions of the input linguistic terms, and this vector is defined as:

$$\boldsymbol{\rho} = [b_{x1,1} \quad b_{x1,2} \quad b_{x1,3} \quad c_{x3,1} \quad a_{x3,2} \quad b_{x3,3}]^T, \quad (16)$$

$J(\boldsymbol{\rho})$  is the objective function with the definition:

$$J(\boldsymbol{\rho}) = \frac{1}{N} \sum_{k=1}^N (y_k(\boldsymbol{\rho}) - y_{k,m}(\boldsymbol{\rho}))^2 = \frac{1}{N} \sum_{k=1}^N (e_{k,m}(\boldsymbol{\rho}))^2, \quad (17)$$

$\boldsymbol{\rho}^*$  is the optimal parameter vector of the fuzzy model which stands for the solution to the optimization problem (15),  $y_k(\boldsymbol{\rho})$  is the output of the SISO process at the  $k^{\text{th}}$  sampling interval,  $y_{k,m}(\boldsymbol{\rho})$  is the

output of the fuzzy model at the  $k^{\text{th}}$  sampling interval,  $e_{k,m}(\mathbf{p}) = y_k(\mathbf{p}) - y_{k,m}(\mathbf{p})$  is the modeling error at the  $k^{\text{th}}$  sampling interval, and  $N$  is the length of the time horizon.

As shown in (Kirkpatrick et al., 1983), (Geman and Geman, 1984), SA algorithms start with a high temperature and an initial solution to the optimization problem. Considering the initial solution represented by the vector  $\varphi$  with the corresponding fitness value  $C(\varphi)$  of the fitness function  $C$ , the next probable solution represented by the vector  $\psi$  is chosen from the vicinity of  $\varphi$ , and it will have the fitness value  $C(\psi)$ . SA algorithms provide a probabilistic framework for solution acceptance. Defining:

$$\Delta C_{\varphi\psi} = C(\varphi) - C(\psi), \quad (18)$$

the probability of  $\psi$  to be the next solution, referred to as  $p_\psi$ , is

$$p_\psi = \begin{cases} 1 & \text{if } \Delta C_{\varphi\psi} > 0, \\ \exp(\Delta C_{\varphi\psi} / \theta) & \text{otherwise,} \end{cases} \quad (19)$$

where  $\theta$  represents the current temperature value specific to the algorithm. If  $p_\psi > r_n$ , where  $r_n$ ,  $0 \leq r_n \leq 1$ , is a randomly selected number, then  $\psi$  will be the new solution. Otherwise, a new solution must be generated. As it can be observed in this framework, there is a valid probability of replacing the current solution with a higher cost solution.

This process is repeated for an a priori set number of steps, and the temperature is next reduced. SA algorithms end when the temperature value is so low that it does not allow any modification of the fitness function, the last value representing the solution to the optimization problem.

Our SA algorithm is implemented in order to solve the optimization problems (9). This SA algorithm is adapted from the class of SA algorithms proposed in (Precup et al., 2012) and applied to the optimal tuning of fuzzy controllers, and the differences between the algorithm proposed in this paper and presented as follows and the SA algorithms given in (Precup et al., 2012) are synthesized in terms of:

- the new SA algorithm is implemented for a significantly larger number of variables of the objective function  $J(\mathbf{p})$  gathered in the vector parameter  $\mathbf{p}$ ,
- the relationship (19) is modified such that to aim the minimization and not the maximization of  $J(\mathbf{p})$ .

Moreover, as defined in (Precup et al., 2011a), two indices are introduced in the algorithm, the success rate  $s_r$  and with the rejection rate  $r_r$ .  $s_r$  focuses the acceleration of the cooling process by forcing a jump in temperature when the minimum value of  $J(\mathbf{p})$  changes for an a priori set number of times at the same temperature level.  $r_r$  is reset only when small values of  $J(\mathbf{p})$  are obtained and not when the temperature is decreasing.

The steps of our SA algorithm, which ensures the minimization of the objective function  $J(\mathbf{p})$  defined in (17), are:

- *Step 1.* Set  $\mu = 0$ ,  $s_r = 0$  and the minimum temperature  $\theta_{\min}$ . Choose the initial temperature  $\theta_0$ .
- *Step 2.* Generate a random initial solution  $\varphi$  and compute its fitness value  $C(\varphi)$ .
- *Step 3.* Generate a probable solution  $\psi$  by disturbing  $\varphi$ , and evaluate the fitness value  $C(\psi)$ .
- *Step 4.* Compute  $\Delta C_{\varphi\psi}$  using (18). If  $\Delta C_{\varphi\psi} \leq 0$ , then accept  $\psi$  as the new solution. Otherwise, set the value of the random parameter  $r_n$ ,  $0 \leq r_n \leq 1$ , and compute  $p_\psi$  according to (19). If  $p_\psi > r_n$ , then  $\psi$  is the new solution.
- *Step 5.* If the new solution is accepted, then update the new solution and  $C$ , increment  $s_r$  and set  $r_r = 0$ . Otherwise, increment  $r_r$ . If  $r_r$  has reached its maximum value  $r_{r\max}$ , the algorithm is stopped; otherwise, continue with step 6.
- *Step 6.* Increment  $s_r$ . If  $s_r$  has reached its maximum value  $s_r$ , go to step 7; otherwise increment  $\mu$ . If  $\mu$  has reached its maximum value  $\mu_{\max}$ , go to step 7; otherwise, go to step 2.
- *Step 7.* Alleviate the temperature according to the temperature decrement rule (Precup et al., 2012):

$$\theta_{\mu+1} = \alpha_{cs} \theta_\mu, \alpha_{cs} = \text{const}, \alpha_{cs} < 1, \alpha_{cs} \approx 1. \quad (20)$$

- *Step 8.* If  $\theta_\mu > \theta_{\min}$  then go to step 3, otherwise the algorithm is stopped indicating that it has reached the end.

The subscript  $\mu$  in this SA algorithm indicates the iteration index. The fitness functions  $C$  implemented in this SA algorithm (dedicated to solving the optimization problem (15)) is the objective functions defined in (16).

Our SA algorithm is mapped onto the optimization problem (15) by means of the following relations between the fitness and objective functions and the parameter vectors as well:

$$J(\mathbf{p}) = C(\psi), J(\mathbf{p}) = C(\varphi), \mathbf{p} = \psi, \mathbf{p} = \varphi. \quad (21)$$

#### 4. EXPERIMENTAL RESULTS

The modeling approach and the Simulated Annealing algorithm presented in the previous sections are applied and exemplified in order to obtain a fuzzy model for the stabilized MLS2EM. A part of the results and implementation details is presented as follows.

For the accepted case study, the values of the maximum consecutive rejections and the maximum success were set to  $r_{r\max} = 100$  and  $s_{r\max} = 50$ , respectively. The initial temperature was chosen as  $\theta_0 = 1$ . The SA algorithm has stopped after 84 iterations, when the temperature value was  $\theta_{84} = 9.04626 \cdot 10^{-0.009}$ . The initial solution is represented by the vector  $\varphi$ :

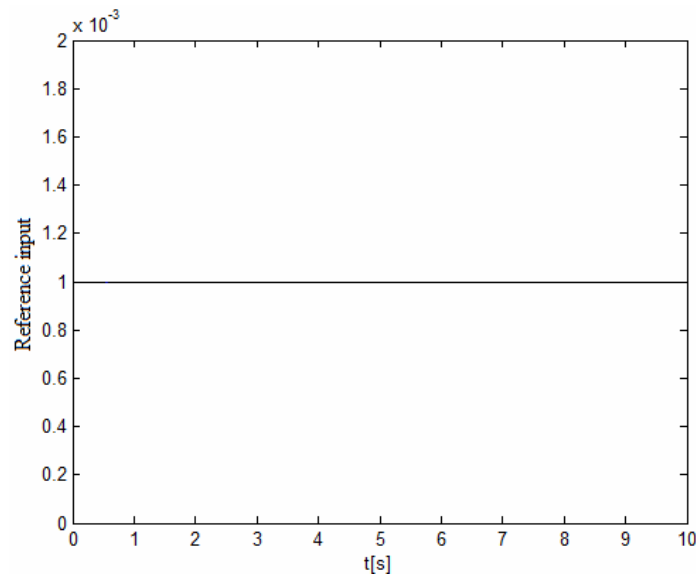
$$\boldsymbol{\rho} = \boldsymbol{\varphi} = [-0.1 \quad 0 \quad 0.1 \quad -1.251 \quad 4.3785 \quad 11.259]^T, \quad (22)$$

and the final solution is represented by the vector  $\boldsymbol{\psi}$ :

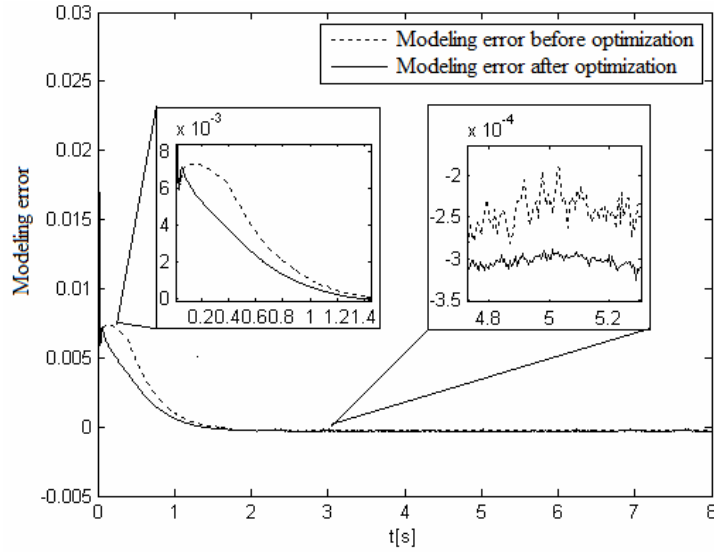
$$\boldsymbol{\rho}^* = \boldsymbol{\psi} = [-0.075 \quad 0.0547 \quad 0.13 \quad -0.63 \quad 4.68 \quad 11.424]^T. \quad (23)$$

The experimental results include the evolutions of the:

- step reference input  $r = 0.01$  at the initial time moment, Figure 3,
- modeling error versus time before and after optimization, Figure 4,
- objective function versus the iteration index in SA algorithm, Figure 5,
- sphere position as output of the T-S fuzzy models, before and after optimization, Figure 6,
- sphere position as output of the SISO process and of the T-S fuzzy models, before and after optimization, Figure 7 and Figure 8, respectively.



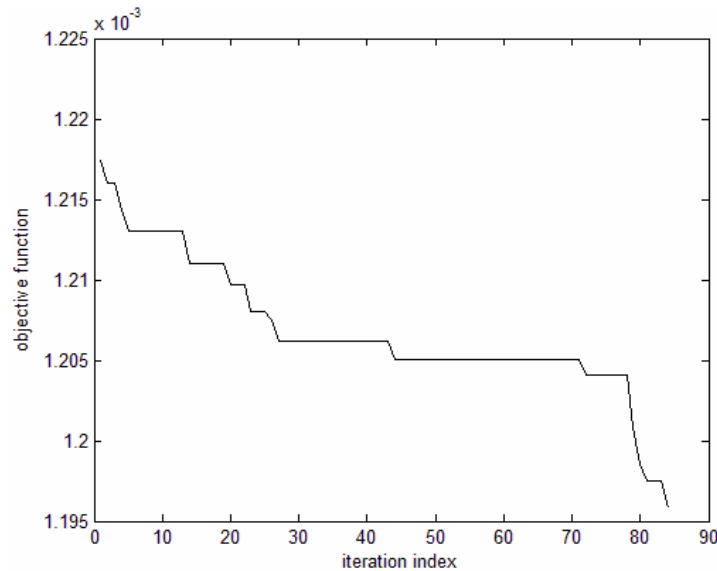
**Figure 3.** Reference input versus time applied to both real-world process and modeled process.



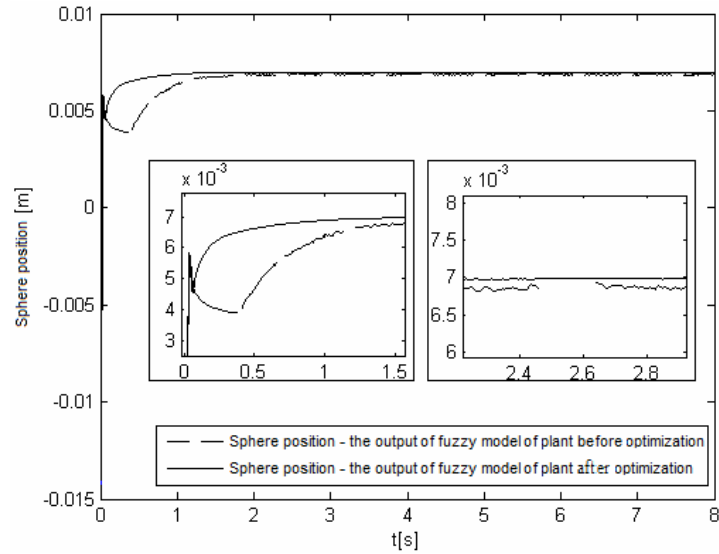
**Figure 4.** Evolution of the modeling error versus time before and after optimization.

Figure 4 shows the performance enhancement ensured by our T-S fuzzy model. The modeling error converges to zero in both cases: before and after optimization, but it can be seen that it converges faster to zero after optimization than before.

The evolution of the objective function versus the iteration index illustrated in Figure 5 shows that the solution to the optimization problem (15) obtained by our SA algorithm ensures a strong decrease of the objective function. Although the minimum of the objective function cannot be guaranteed, Figure 5 highlights that the improvement can continue by considering a larger number of iterations.



**Figure 5.** Evolution of the objective function versus the iteration index in SA algorithm.



**Figure 6.** Real-time experimental results of modeled process before and after optimization with SA algorithm.

Figure 6 points out that the evolution of the sphere as output of our T-S fuzzy model after applying of the SA algorithm (the straight line) is faster, with a smaller settling time and an aperiodically evolution. These performance indices are much better compared to those of the initial T-S fuzzy model, i.e., before the application of the SA algorithm (the interrupted line). The straight line also shows that the desired sphere position,  $y_k = 0.007$  m, is reached.

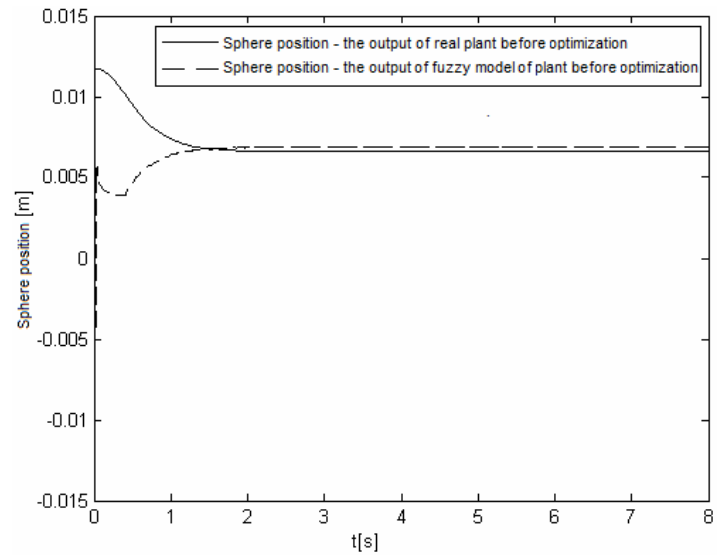


**Figure 7.** Real-time experimental results of SISO process and of T-S fuzzy model of process before optimization with SA algorithm.

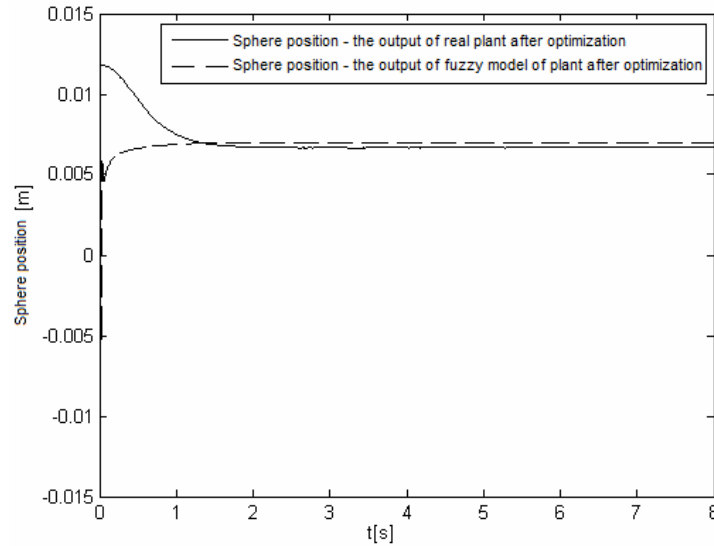


**Figure 8.** Real-time experimental results of SISO process and of T-S fuzzy model of process after optimization with SA algorithm.

It can be seen that the behavior of the sphere in Figures 7 and 8 in both cases (SISO process and T-S fuzzy model) before (the straight line) and after optimization with SA algorithm (the interrupted line) have a similar evolution. In the second case, the response is faster, with a smaller settling time and an aperiodically evolution. These performance indices are much better compared to those of the initial T-S fuzzy model. However, the results can be different for other applications (Ruano et al., 2003), (Hermann et al., 2009), (Milojković et al., 2010), (Kovács et al., 2011), (Kumbasar et al., 2011), (Iwasaki et al., 2012), (Liu et al., 2012), (Papadopoulos et al., 2012).

## 5. CONCLUSIONS

The paper has proposed an approach to the fuzzy modeling of magnetic levitation systems. This approach is based on the implementation of SA algorithms to optimize the parameters of T-S fuzzy models initially obtained in terms of the modal equivalence principle.

A new T-S fuzzy model of an MLS2EM laboratory equipment is offered. The new modeling approach is important because it is applicable with adequate but not complicated generalizations to a wide category of industrial applications. Similar other T-S fuzzy models can be obtained in order to be further used in the T-S fuzzy controller design and tuning.

## ACKNOWLEDGEMENTS

This work was supported by a grant in the framework of the Partnerships in priority areas - PN II program of the Romanian National Authority for Scientific Research ANCS, CNDI - UEFISCDI, project number PN-II-PT-PCCA-2011-3.2-0732.

## REFERENCES

- Babu Devasenapati, S. Ramachandran, K.I., 2011, Hybrid fuzzy model based expert system for misfire detection in automobile engines. *International Journal of Artificial Intelligence* **7**, 47–62.
- Baranyi, P., Yam, Y., Várkonyi-Kóczy, A., Patton, R.J., 2003, SVD based reduction to MISO TS fuzzy models. *IEEE Transactions on Industrial Electronics* **50**, 232–242.
- Geman, S., Geman, D., 1984, Stochastic relaxation, Gibbs distribution and the Bayesian restoration in images. *IEEE Transactions on Pattern Analysis and Machine Intelligence* **6**, 721–741.
- Haber, R.E., del Toro, R.M., Gajate, A., 2010, Optimal fuzzy control system using the cross-entropy method. A case study of a drilling process. *Information Sciences* **180**, 2777–2792.
- Hermann, G., Kozłowski, K.R., Tar, J.K., 2009, Design of a planar high precision motion stage. In: *Robot Motion and Control 2009*, K.R. Kozłowski (Ed.), Lecture Notes in Control and Information Sciences, Springer-Verlag, Berlin, Heidelberg, **396**, 371–379.
- Hong S.-K., Langari, R., Joh J., 1997, Fuzzy modeling and control of a nonlinear magnetic bearing system. *Proceedings of the 1997 IEEE International Conference on Control Applications*, Hartford, CT, USA, 213–218.
- Inteco Ltd, 2008, *Magnetic Levitation System 2EM (MLS2EM)*, User's Manual (Laboratory Set), Krakow, Poland: Inteco Ltd.
- Iwasaki, M., Seki, K., Maeda, Y., 2012, High-precision motion control techniques: A promising approach to improving motion performance. *IEEE Industrial Electronics Magazine* **6**, 32–40.
- Johanyák, Z.C., 2010, Survey on five fuzzy inference-based student evaluation methods. In: *Computational Intelligence in Engineering*, I.J. Rudas et al. (Eds.), Studies in Computational Intelligence, Springer-Verlag, Berlin, Heidelberg, **313**, 219–228.
- Kirkpatrick, S., Gelatt, Jr., C.D., Vecchi, M.P., 1983, Optimization by simulated annealing. *Science* **20**, 671–680.
- Kovács, L., Benyó, B., Bokor, J., Benyó, Z., 2011, Induced  $L_2$ -norm minimization of glucose-insulin system for type I diabetic patients. *Computer Methods and Programs in Biomedicine* **102**, 105–118.
- Kumbasar, T., Eksin, I., Guzelkaya, M., Yesil, E., 2011, Interval type-2 fuzzy inverse controller design in nonlinear IMC structure. *Engineering Applications of Artificial Intelligence* **24**, 996–1005.
- Lee, T.-E., Su, J.-P., Yu, K.-W., 2007a, Implementation of the state feedback control scheme for a magnetic levitation system. *Proceedings of 2<sup>nd</sup> IEEE Conference on Industrial Electronics and Applications (ICIEA 2007)*, Harbin, China, 548–553.
- Lee, Y.-H., So, M.-O., Jin, G.-G., 2007b, T-S fuzzy modeling and model-based fuzzy control for nonlinear systems using a RCGA technique. *Proceedings of International Conference on Control, Automation and Systems (ICCAS 2007)*, Seoul, Korea, 132–136.

- Liu, J., Zanchetta, P., Degano, M., Lavopa, E., 2012, Control design and implementation for high performance shunt active filters in aircraft power grids. *IEEE Transactions on Industrial Electronics* **59**, 3604–3613.
- Michino, R., Tanaka, H., Mizumoto, I., 2009, Application of high gain adaptive output feedback control to a magnetic levitation system. *Proceedings of ICROS-SICE International Joint Conference (ICCAS-SICE 2009)*, Fukuoka, Japan, 970–975.
- Milojković, M., Nikolić, S., Danković, B., Antić, D., Jovanović, Z., 2010, Modelling of dynamical systems based on almost orthogonal polynomials. *Mathematical and Computer Modelling of Dynamical Systems* **16**, 133–144.
- Papadopoulos, K.G., Tselepis, N.D., Margaritis, N.I., 2012, Revisiting the Magnitude Optimum criterion for robust tuning of PID type-I control loops. *Journal of Process Control* **22**, 1063–1078.
- Precup, R.-E., David, R.-C., Petriu, E.M., Preitl, S., Rădac, M.-B., 2012, Fuzzy control systems with reduced parametric sensitivity based on simulated annealing. *IEEE Transactions on Industrial Electronics* **59**, 3049–3061.
- Precup, R.-E., David, R.-C., Petriu, E.M., Rădac, M.-B., Preitl, S., Fodor, J., 2011a, Evolutionary optimization-based tuning of low-cost fuzzy controllers for servo systems. *Knowledge-Based Systems* DOI: 10.1016/j.knosys.2011.07.00.
- Precup, R.-E., Preitl, S., Rădac, M.-B., Petriu, E.M., Dragoș, C.-A., Tar, J.K., 2011b, Experiment-based teaching in advanced control engineering. *IEEE Transactions on Education* **54**, 345–355.
- Ruano, A.E., Fleming, P.J., Teixeira, C.A., Rodríguez-Vázquez, K., Fonseca, C.M., 2003, Nonlinear identification of aircraft gas-turbine dynamics. *Neurocomputing* **55**, 551–579.
- Satoh, Y., Nakamura, H., Nakamura, N., Katayama, H., Nishitani, H., 2009, Robust adaptive control of nonlinear systems with convex input constraints: Case study on the magnetic levitation system. *Proceedings of ICROS-SICE International Joint Conference (ICCAS-SICE 2009)*, Fukuoka, Japan, 4411–4416.
- Škrjanc, I., Blažič, S., Agamennoni, O.E., 2005, Identification of dynamical systems with a robust interval fuzzy model. *Automatica* **41**, 327–332.
- Vaščák, J., Madarász, L., 2010, Adaptation of fuzzy cognitive maps – a comparison study. *Acta Polytechnica Hungarica* **7**, 109–122.
- Wang, D., Wang, F., 2010, Design of PDC controller based on T-S fuzzy model for magnetic bearing of high-speed motors. *Proceedings of 3<sup>rd</sup> IEEE International Conference on Computer Science and Information Technology (ICCSIT 2010)*, Chengdu, China, **1**, 602–606.
- Xi, Z., Feng, G., Hesketh, T., 2011, Piecewise sliding-mode control for T-S fuzzy systems *IEEE Transactions on Fuzzy Systems* **19**, 707–716.

Xiu, J., Xia, C.-L., 2007, Modeling of switched reluctance motor based on GA optimized T-S type fuzzy logic. *Proceedings of Fourth International Conference on Fuzzy Systems and Knowledge Discovery, (FSKD 2007)*, Haikou, Hainan, China, **4**, 186–191.

Yang, Z.-J., Fukushima, Y., Kanae, S., Wada, K., 2009, Robust non-linear output-feedback control of a magnetic levitation system by k-filter approach. *IET Control Theory & Applications* **3**, 852-864.

Yongzhi, J., Kunlun, Z., Jian, X., 2011, Modeling of gap sensor for high-speed Maglev train based on fuzzy neural network. *Proceedings of Eighth International Conference on Fuzzy Systems and Knowledge Discovery (FSKD 2011)*, Shanghai, China, **1**, 650–654.

Yu, G.-R., Huang, Y.-J., T-S Fuzzy control of magnetic levitation systems using QEA. *Proceedings of Fourth International Conference on Innovative Computing, Information and Control (ICICIC 2009)*, Kaohsiung, Taiwan, 1110–1113.

Yu, S.-S., Wu, S.-J., Lee, T.-T., 2003, Application of neural-fuzzy modeling and optimal fuzzy controller for nonlinear magnetic bearing systems. *Proceedings of IEEE/ASME International Conference on Advanced Intelligent Mechatronics, (AIM 2003)*, Kobe, Japan, **1**, 7–11.